Advances in Natural Sciences:
Nanoscience and Nanotechnology

Verification of resistance to three mediated microbial strains and cancerous defense against MCF7 compared to HepG2 through microwave synthesized plant-mediated silver nanoparticle

To cite this article: W I Abdel-Fattah *et al* 2015 *Adv. Nat. Sci: Nanosci. Nanotechnol.* **6** 035002

OPEN ACCESS

IOP Publishing | Vietnam Academy of Science and Technology Advances in Natural Sciences: Nanoscience and Nanotechnology

Adv. Nat. Sci.: Nanosci. Nanotechnol. **6** (2015) 035002 (13pp) doi:10.1088/2043-6262/6/3/035002

Verification of resistance to three mediated microbial strains and cancerous defense against MCF7 compared to HepG2 through microwave synthesized plant-mediated silver nanoparticle

W I Abdel-Fattah[1,*], M M Eid[2], M F Hanafy[3], M Hussein[3], Sh I Abd El-Moez[4], S M El-Hallouty[5] and E Mohamed[3]

[1] Biomaterials Ceramics and Ceramics/Polymer Composites, Biomaterials Department, National Research Centre (NRC), Tahrir Street, Dokki, Cairo, 12311, Egypt
[2] Spectroscopy Department, Physics Division, National Research Center (NRC), Tahrir Street, Dokki, Cairo, 12311, Egypt
[3] Biophysics Department, Faculty of Science, Zagazig University, 44519, Egypt
[4] National Research Center (NRC), Tahrir Street, Dokki, Cairo, 12311, Egypt
[5] Pharmacognosy Department, National Research Centre, Tahrir Street, Dokki, Cairo, 12311, Egypt

E-mail: nrcfifi@yahoo.com

Received 24 December 2014
Accepted for publication 18 March 2015
Published 14 April 2015

Abstract

The antimicrobial and anticancer efficiencies of green synthesized silver nanoparticles (AgNPs) through biogenic extracts were assessed on three bacterial strains and two cancer cell lines. Bio-synthesized AgNPs were achieved through domestic microwave generator for obtaining extracts from Asian nuts and Egyptian blackberry fruits. Surface plasmon resonance (SPR) ~435 nm demonstrated AgNPs earlier formation by the fruit extract. Capping by triglycerides/almond and phenols/berry extracts were responsible for the reduction proved by FTIR. XRD calculated particle sizes were 18 and 42 nm while TEM sizes are 24.5 and 21.5 nm for AgNPs from almond nut and blackberry fruits extracts (Alm.N.Ext. and BB.F.Ext.), respectively. Ag 3d5/2 was recorded at 368.12 eV for both samples through XPS. The monodispersed AgNPs recorded 0.727 and 0.5 polydispersity indices (PdI) for almond/Ag and berry/Ag, respectively. Zeta potential ~ −31 and −13.2 for the same sequence confirmed the higher stability of the former. Reaction kinetics confirmed the advantage of fruit extract consuming only six minutes compared to nuts, consuming twice. Bactericidal effect of the extracts seldomly presented remarkable inhibition compared to extracts/Ag against the three species. In addition, Alm.N.Ext. showed the highest inhibition against staphylococcus aureus (*S. aureus*) at 4 mM. The anti-cancerous effect of Ag/berry against HepG2 is stronger than Ag/almond, and similarly for MCF7.

Keywords: bactericidal/anticancer approach, Ag-NPs, Green chemistry, spectral analysis, zeta-potential
Classification numbers: 2.04, 2.05, 4.02

* Author to whom any correspondence should be addressed.

1. Introduction

Being a multidisciplinary area of science and technology recently developed on the basis of the synthesis of the achievements of physics, chemistry, biomedical sciences as well as of the information technology, nanotechnology is one of the prior areas of science and technology of all advanced countries in the world and also of many developing countries [1–3].

Nanobiotechnology links biological principles with physicochemical tools to create nanoparticles with specific functions. It offers an economic use for chemical and physical avenues for nanoparticles production [4]. The incorporation of nanoparticles with biogenic molecules has led to the evolution of several diagnostic devices, contrasting agents and principal routes in cancer therapy [5].

Synthesis is carried out by numerous physical and chemical techniques, laser ablation, pyrolysis, chemical or physical vapor deposition, sol-gel, and lithography electrodeposition. However, most of them are expensive requiring toxic solvents [6]. Considerable efforts to manipulate environmentally friendly methods for the synthesis of noble metal nanoparticles have been conducted [7]. These are usually accomplished by the utilization of plant leaves or fruit extracts [8] and bio-organisms [9]. Also, green methods have the privilege of being fast and efficient leading to the production of crystalline nanoparticles. A diversity of shapes as spheres, rods, prisms, plates, needles, leaves or dendrites are thus achieved [10]. Microwave heating significantly decreases response times, increases product yields and improves product's purities by minimizing unwanted side reactions compared to traditional methods. Its enhanced chemistry depends on the perfect heating of materials by 'microwave dielectric heating' effects. Compared to traditional courses, microwave assisted synthesis is faster, leading to particles with an average size of 12 nm [11].

The health advantages of almond nuts are related to their effects on serum lipids and cardiovascular attacks. These benefits are attributed to their content of mono- and polyunsaturated fatty acids. Moreover, their antioxidant activities are related to polyphenols, tocopherols as well as the phytosterols that reduce cholesterol effects [12–15]. On the other hand, berry fruits offer many protective effects that are linked to their phenolic compounds, including flavonoids and anthocyanins [16–21]. The later constitute the essential group of phenolic compounds in raspberry where the content of ellagic acid is high, but less than anthocyanins [22–25].

Escherichia coli (*E. coli*) are bacteria population of the gastrointestinal tract of humans and animals [26], they are either commensals or pathogenic [27]. *E. coli* O157 represents isolates that are Shiga-like toxin producers and are zoonotic agents causing severe diseases like diarrhea, hemorrhagic colitis (HC) and hemolytic uraemic syndrome (HUS) [28]. *Staphylococcus aureus* (*S. aureus*) is a leading cause of food poisoning resulting from the consumption of contaminated food with staphylococcal enterotoxins. Different foods are suitable media for *S. aureus* such as fresh meat and meat products [29], raw milk, dairy products and ready-to-eat food [30]. Enterotoxins are highly thermostable, usual cooking and pasteurization cannot totally inactivate them causing food poisoning [31]. The onset of symptoms depends on the amount of enterotoxin ingested. Classic staphylococcal enterotoxins (SEs) antigens have been identified as SEA, SEB, SEC1, SEC2, SEC3, SED [32]. The Candida species present the most frequent isolated organisms among the fungal [33, 34]. These represent groups of unicellular opportunistic organisms, ever present in the natural surroundings of dairy cattle. They are normal inhabitants of the skin of the udder and teats and are existing in few numbers. They can invade mammary glands causing clinical mastitis. They are characterized by pain, prolonged fever, tenderness, an inflammatory reaction in the mammary glands and associated lymph nodes leading to milk yield and quality reductions [35]. Some intramammary fungal infections such as A. fumigants and Candida Sp may result in death of affected animals [36, 37].

In Egypt the most common cancer among females is breast cancer estimated to be accounting for 37.7% of their total with 12,621 new cases in 2008. It is the leading cause of cancer-related mortality accounting for 29.1% of their total with 6546 deaths (Egypt National Cancer registry Demitta Profile, 2009). On the other hand, liver cancer death in Egypt reached 5354, i.e., 1.47% of total death according to the latest WHO 9 April 2010. Egypt is ranked 51 worldwide considering the age adjusted death rate is 9.79 per 100 000 of the population.

A green approach was manipulated, in the present work, to produce extracts from two different plant sources applying microwave energy to achieve mono-dispersed silver nanoparticles (AgNPs). Extracts were obtained from an Asian nut: almond and a particular traditional Egyptian fruit: the blackberry. Each extract was used separately for the synthesis of AgNPs using the microwave device for several exposure times but at a constant power. The achieved nanoparticles at the selected optimal conditions from each source were subjected to spectral analyzes of ultraviolet-visible (UV–vis), Fourier transform infrared (FTIR), x-ray diffraction (XRD), and x-ray photoelectron spectroscopy (XPS). The nanoparticles shapes and sizes were defined using high-resolution transmission electron microscopy/selected area electron diffraction (HR-TEM/SAED), zeta potential and dynamic light scattering (DLS). Their antimicrobial effects were compared for three strains: gram-negative bacteria (*E. coli*), gram-positive bacteria (enterotoxigenic *S. aureus*) and mycotic strain (*C. albicans*). Anticancer efficiencies were performed against two cell lines, MCF7 (human breast carcinoma) and HepG-2 (human liver carcinoma).

2. Materials and methods

2.1. Synthesis

Almond nuts (prunusamygdalus) and the berry fruits were used. The microwave was applied for the processing of extracts for several minutes in a cyclic mode of (on 5 s, off

Table 1. Notation of almond nuts and blackberry fruits extracts and with AgNP post μ-wave treatment.

Resources	Received dried	Extract post μ-wave	Extract/silver post μ-wave
Almond nut	Alm.N	Alm.N.Ext	Alm.N.Ext/Ag
Blackberry fruit	BB.F	BB.F.Ext	BB.F.Ext/Ag

5 s) to prevent intense boiling as well as aggregation. Proper filter paper size was used to obtain extracts for the reduction of Ag ions into Ag^{o}. 10 g of each source along with 50 ml of bidistilled water in 100 ml erlenmeyer flask were subjected to microwave heating for several periods before decantation. The extracts were filtered and stored in the fridge for further synthesis experiments. Silver nitrate ($AgNO_3$) (Sigma-Aldrich Chemicals) was used in several concentrations. The nuts, fruits, and their extracts pre- and post microwave treatment for the experienced conditions are presented (table 1).

2.2. Characterization

UV–vis spectral analyzes were performed (JASCO, V-530 spectrophotometer) at a resolution of 1 nm. FTIR spectroscopic characterization was executed (Perkin Elmer FTIR spectrophotometer) to investigate the influence of the functional groups of either extract on nanoparticles development through reduction of silver ions and to assess their surface structures. The dried extracts and silver nanoparticles were mixed with KBr powder semi-quantitatively (1–200 mg). XRD analyses were recorded on a Bruker D-8 powder x-ray diffractometer using Cu-Kα radiation ($\lambda = 0.15418$ nm) within θ range of 20°–90° with a step of 0.02°. The exposed silver surface species were determined by XPS on an Axis Ultra DLD spectrometer with Al-Kα radiation ($h\nu = 1486.71$ eV) and resolution of energy of 0.48 eV. The peak positions were corrected for sample charging by setting the C 1 s binding energy at 284.8 eV. XPS analyses were conducted at 150 W and pass energy of 16 eV. Techno Philips HR-TEM, 200 kV, microscopic studies were performed to characterize sizes, shapes and morphological features of AgNPs. The HR-TEM is supplemented with the SAED facility. Energy-dispersive analysis of x-rays (EDAX) analyses were done using FEI Quanta 200 ESEM. Particle size distribution was estimated using a Zetasizer 1000 HS (Malvern Instruments, UK). The light scattering fluctuations due to Brownian motion of the particles were analyzed by photon correlation spectroscopy. Measurements were performed at 25 °C with an incident wavelength of 633 nm and a 173° backscattering angle at pH 7.0. Clear disposable zeta-potential cells (one cm path length) were rinsed with ethanol, followed by deionized water prior to sample loading. Monitoring light scattering was performed at 25 °C with a 90° angle. Particle size distribution was achieved at a fixed refractive index of the respective formulation, and particles stability was assessed by zeta potential. The ranges of size distribution were measured (a particle size analyzer PSA: Malvern Zeta Sizer Nano ZS). The dynamic light scattering (DLS) analyses were performed at pH of 7.0 ± 0.2.

2.3. Antimicrobial efficiency of bio-silver-nanoparticles

The antimicrobial activities were carried out using the agar well diffusion method [38–40] applying different concentrations of the tested nanoparticles (table 4). The method is a qualitative technique for studying the antimicrobial activities of the nanoparticles within almond or blackberry extracts. The tested bacterial strains were: gram-negative (*E. coli* O157 ATCC 700728), gram-positive (enterotoxigenic *S. aureus* ATCC 13565) and mycotic strain (*C. albicans* ATCC). Dimethyl sulphoxide (DMSO) was used as control. Müller–Hinton agar plates (negative control) were inoculated with bacterial strains. On the other hand, Sabouraud dextrose agar plates were inoculated with fungal strains in concentrations equivalent with 0.5 McFarland for bacterial strains and 2×10^5 and streaked onto the agar plates using sterile swabs. Then 80 μl of the tested samples were placed into the wells under sterile conditions. Plates were incubated aerobically at 37 °C in 24 h for bacterial growth and 28 °C in 48–72 h for fungal growth. Inhibition zones were measured (mm), and experiments were carried out in triplicates.

2.4. Anticancer activities

2.4.1. Cell culture. MCF7 (human breast carcinoma) and HepG-2 (human liver carcinoma) cell lines were used (Karolinska Institute, Stockholm, Sweden). Cells were maintained in RPMI 1640 medium, (LonzaBiowahittkar, Belgium). Additionally, 1% antibiotic–antimycotic mixture (10 000 U mL−1 potassium penicillin, 10 000 μg mL^{-1} streptomycin sulfate, 25 μg mL^{-1} amphotericin B, and 1% L-glutamine (Biowest, USA) supplemented the media.

2.4.2. MTT cytotoxicity assay. This assay was used to investigate cell viability [3-(4, 5-dimethylthiazol-2-yl)-2,5-diphenyltetrazolium bromide] (MTT) (Bio Basic Canada Inc., Canada). The reaction depends on the mitochondrial reduction of yellow MTT into purple formazan. A sterile laminar air flow cabinet biosafety class II level (Baker, SG403INT, Stanford, ME, USA) was used for performing all the preceding steps. Incubations were done at 37 °C in 5% CO_2 incubator and humidified atmosphere (Sheldon, TC2323, Cornelius, OR, USA). Cells were seeded into 96-well microtiter plastic plates at the concentration of (104 cells per well) and allowed to adhere for 24 h. Media were aspirated and fresh media (without serum) were added to the cells with various concentrations of the test compounds (100, 50, 25, 12.5, 6.25, 3.12, 1.56, and 0.78 μg mL^{-1} in dimethyl sulfoxide) and were further incubated for 48 h. Media were aspirated, and 40 μL MTT salt (2.5 μg mL^{-1}) were added to each well and incubated for additional 4 h. Sodium dodecyl sulfate (SDS) 200 μL of 10% were added to each well to stop the reaction and dissolve any formed formazan crystals then incubated overnight at 37 °C. The amounts of formazan product were measured at 595 nm with a reference

wavelength of 620 nm as a background using a microplate reader (Bio-Rad Laboratories, model 3350, USA). For the untreated cells (negative control), media were added instead of the test compounds. Adrinamycin® (doxorubicin) (Mr = 579.9) was used as a positive control at a known cytotoxic natural agent giving 100% inhibition. The vehicle used for dissolution of the tested compounds was dimethyl sulfoxide (DMSO) and its final concentration on the cells <0.2%.

2.4.3. Statistical analysis. Probit analysis using a simple t-test (SPSS statistical analysis software package/version 11.0, SPSS Inc., (IL), Chicago, USA) was used to calculate LC50 for the samples and the negative control (cells with vehicle).

3. Results and discussion

The successive formation of AgNPs turned colorless $AgNO_3$ solutions to brown or reddish yellow to dark red the higher the duration of microwave irradiation. The brown color was due to the excitation of the silver surface plasmon resonance (Ag SPR) vibrations [41]. Samples abbreviations are given in table 1.

The broadness of UV–vis spectra proved wide particle size distribution. The absorption peaks grew sharper in parallel with the enhanced homogeneity of the particles [42]. The sizes of silver nanoparticles were reported to have a linear correlation with the peak intensities [43]. The characteristic (Ag/SPR) bands are recorded at ~435 nm and 439 nm for Alm.N.Ext./Ag and BB.F. Ext./Ag, respectively (figure 1).

Microwave exposure time less than 14 min shifted almond surface plasmon resonance (SPR) peak to a higher wavelength ~435 nm but with smaller intensities (figure 1(a)) due to inferior AgNPs formation. Conversely, reducing the microwave exposure time shifts the wavelength to a lower value ~437 nm, for the berry (at 5 min exposure, figure 1(b)). The absorption peak at 220 nm refers to the negative control, i.e. $AgNO_3$. At 280 nm, the peak is attributed to tyrosine and tryptophan residues of proteins in the extracts. Any peak at 260 nm could be due to free amino acids or carbohydrates (data not shown). The reduced band width and higher band intensity proved enlarged particle size. The effect of $AgNO_3$ concentrations on the final silver nanoparticles will be discussed (running work). The present samples were exposed to the time of 600 s and 840 s for Alm.N.Ext./AgNPs samples while only 360 s were sufficient for BB.F.Ext./AgNPs. The size, shape, and the surrounding environment of the synthesized AgNPs changed when the solutions were microwave irradiated for more than 120 s [44].

The kinetics of reduction processes demonstrated that the rate of formation of AgNPs was faster using blackberry extracts compared to those almond nuts. Changes of relationship between the exposure times (t) in minutes and $\ln A_t/A_0$ fit a linear correlation, where A_0 and A_t are absorbance intensities at initial time and exposure time t, respectively. The calculated slope of the linear equation for blackberry reduction rate was higher (R = 0.429 min) in comparison with the linear equation for almond nuts (R = 0.145 and 0.095 min) at extraction time of 14 min and 12 min, respectively (figure 2).

Fourier transform infrared (FTIR) spectra of the extracts and extracts/Ag samples (figure 3) prove the dual role of the plant extracts as a bio-reductant and capping agents. The 3467 cm^{-1} band could be attributed to glyceride carbonyl because, the one at 3007 cm^{-1} is due to the C-H stretching vibration. The glyceride carbonyl group changed to 3423 and 3359 cm^{-1} for the Alm.N.Ext. and Alm.Ext./Ag, respectively. Several bands at 1463, 1378, 1239 and 1163 cm^{-1} are due to the fingerprint of fatty acids while that at 1097 cm^{-1} is due to C=C (figure 3(c)) [45]. The carbonyl triglyceride bands for the extract and the extract/AgNP moved to 1617 and 1572 cm^{-1}, while the 1463 cm^{-1} band changed to 1406 and 1478 cm^{-1} for the Alm.Ext. and Alm.Ext/Ag, respectively (figure 3(a)). Since 1378 cm^{-1} band moved to 1336 cm^{-1} for the Alm.Ext./Ag its absence in Alm.N.Ext. proved its responsibility. The fatty acids group that should be at 1163 cm^{-1} moved to 1139 cm^{-1} for the Alm.N.Ext. and disappeared for the Alm.Ext/Ag. The C=C band changed its position from 1097 to 1053 and 1057 cm^{-1} for the same sequence. The carbonyl group vibration at 1746 cm^{-1} recognized the triacylglycerols.

The enhanced intensities of five IR bands at 3423, 1622, 1411, 1053 and 998 cm^{-1} for Alm.Ext./Ag demonstrated their contribution in the stability of the AgNP. The C-H bending at 992 cm^{-1} in the Alm.Ext. changes from a kink to a shoulder for the Alm.Ext./Ag proving, therefore, its involvement in the reduction of Ag^+ to Ag^o and a new band appeared at 998 cm^{-1}. The bands at 3383 and 2855 cm^{-1} are attributed to phenolic O-H while that at 2926 cm^{-1} is due to C-H bond. The bands at 1745 and 1413 cm^{-1} are assigned to C=O (figure 3(c)). The O-H band moved to 3418 and 3348 cm^{-1} for the former and latter respectively (figure 3(b)). The carbonyl band at 1745 cm^{-1} changed its position to 1631 and 1591 cm^{-1} for the same sequence while the C=O band at 1413 cm^{-1} showed blue move to 1341 cm^{-1}. Moreover, the band at 1066 shifted to 1008 cm^{-1} for the berry extract/AgNP. Additionally, the band at 1637 cm^{-1} is related to the amide bond (C=O) while that at 1256 cm^{-1} recognizes C-O and 1146 cm^{-1} due to C-O-C. The O-H band at 3348 cm^{-1} and the C-O-C-band at 1008 cm^{-1} have increased intensities compared to the extract proving, therefore, their responsibility for AgNPs stability [46]. The C-OH at 1146 cm^{-1} of the fruit turned to only a shoulder at 1149 cm^{-1} and 1089 cm^{-1} for the extract and Ext.F./Ag, respectively. Its appearance proves the O-H group involvement in the reduction of Ag^+ to Ag^o [47]. The oxidation of C=O increases as the two bands at 1745 and 1637 cm^{-1} merge into one broad band for the Ext.F./Ag [48]. Therefore, Ag^+ reduction to AgNPs by the OH of the C-OH group at 1066 cm^{-1} is responsible [49–51]. The OH band for the dried (black) AgNP is sharper than samples dried by freeze drying (blue).

The dried nanoparticles possessed XRD patterns for Alm. N.Ext./AgNP and BB.F.Ext/AgNP shown in (figures 4(a) and (b)). Four peaks recorded at 38.21, 44.31, 64.71 and 77.81°

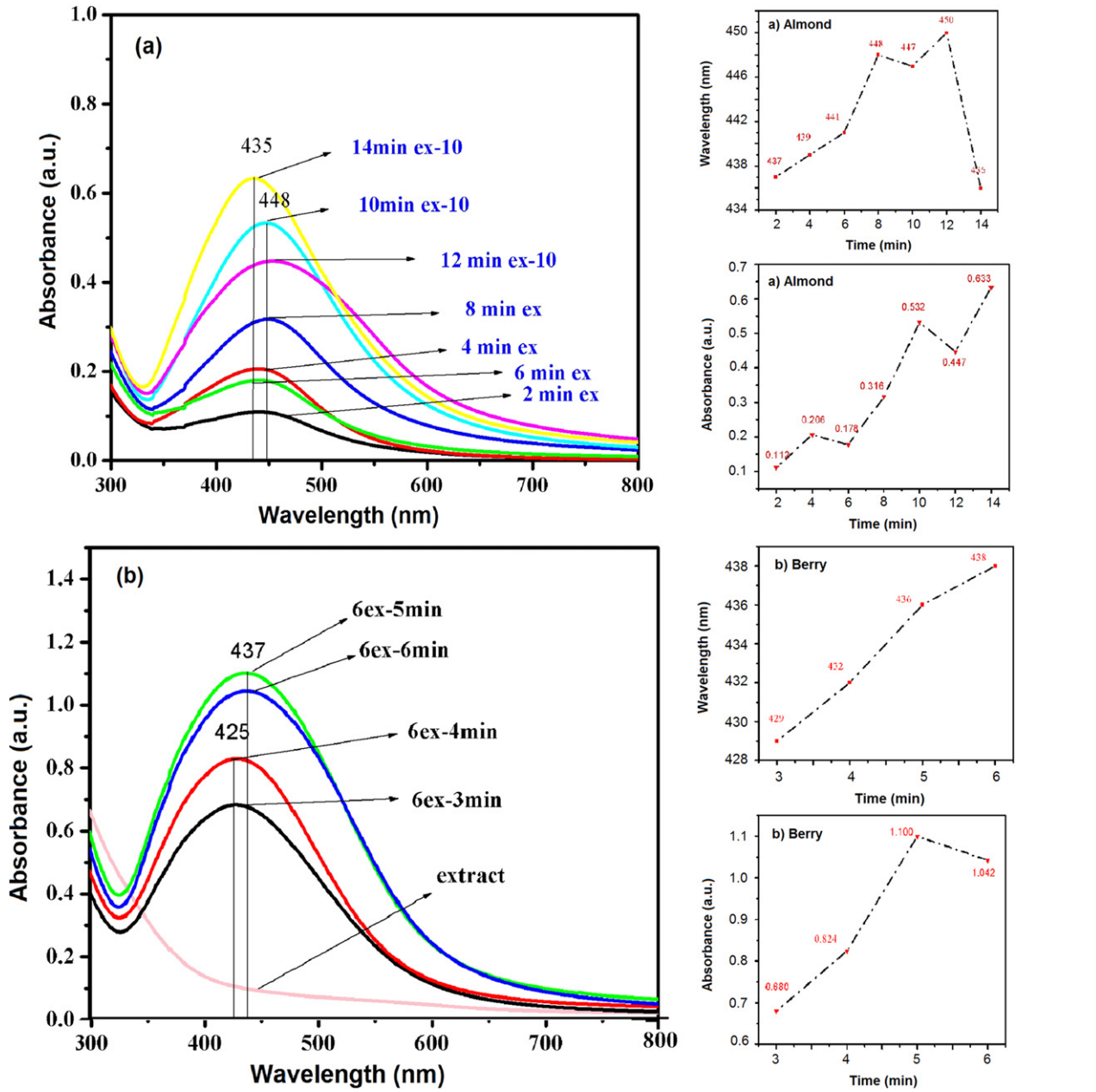

Figure 1. UV–vis absorption spectra of the silver nanoparticles prepared from (a) almond nuts extracts and (b) blackberry extract.

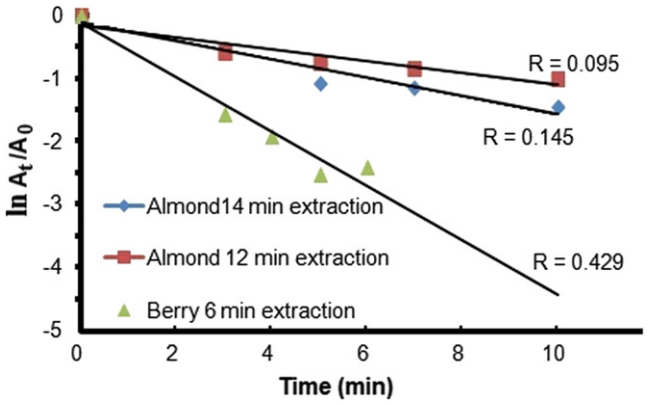

Figure 2. The kinetics of AgNPs formation from almond and berry extracts.

within the 2θ range 30–80° are characterizing Ag. They are indexed to (111), (200), (220) and (311) for fcc structure of metallic silver (JCPDS file No 43-0641) and, therefore, proved pure crystalline silver. The ratio between the (200) and (111) diffraction peak intensities is 0.37, which is lower than the conventional bulk intensity (0.52). Therefore, the (111) plane is the predominant orientation [52–56]. Similar results are recorded for BB.F.Ext./AgNPs. The quasi-spherical morphology predominantly has the {100} along with the {111} facet. The average nanocrystallite sizes were calculated using the Debye-Scherrer's formula $D = K\lambda/(\beta \cos\theta)$, where D is crystallite size, $K = 0.94$ is shape factor and λ is wavelength of Cu-Kα radiation. The average crystallite sizes of the Ag NPs are 18 and 42 nm for Alm.N.Ext./Ag and BB.F.Ext./Ag, respectively [57].

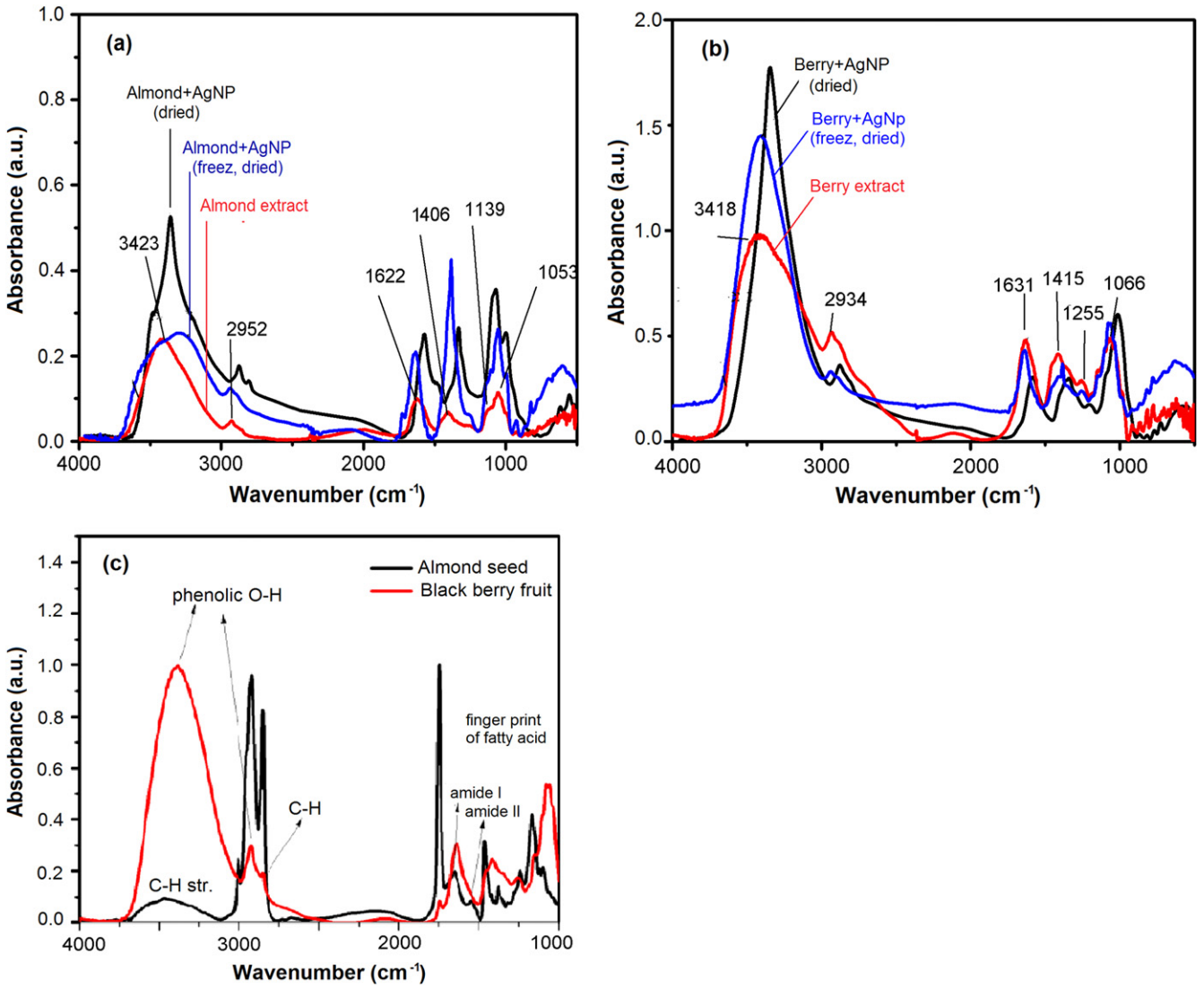

Figure 3. FTIR spectra for the silver nanoparticles synthesized from microwave treated extracts of (a) almond,(b) blackberry and (c) their control.

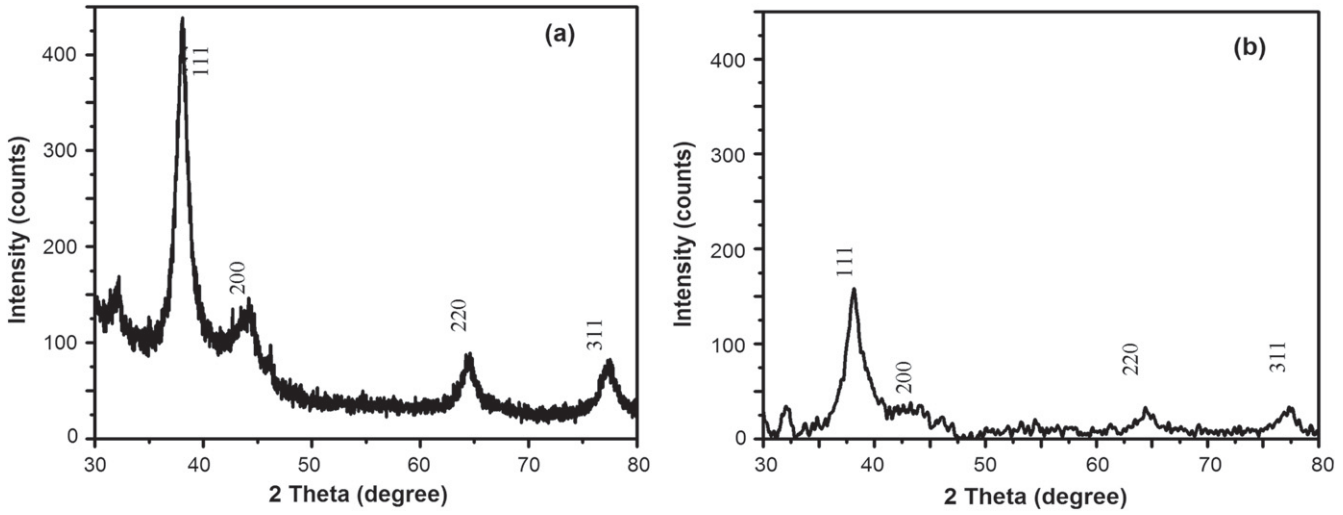

Figure 4. XRD patterns of the silver nanoparticles synthesized in (a) almond extract and (b) blackberry extract utilizing microwave route at optimum conditions.

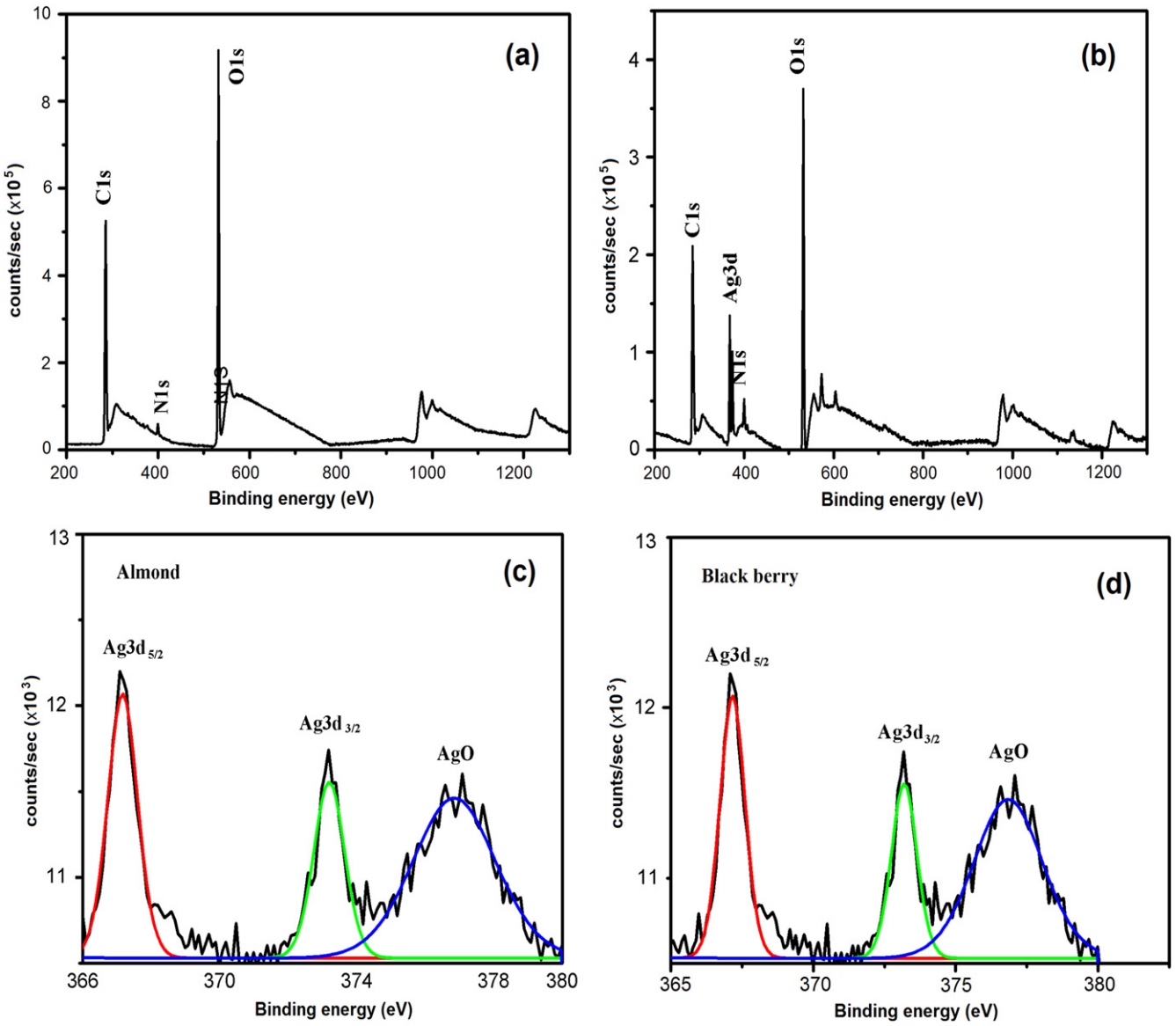

Figure 5. XPS survey for the silver nanoparticles synthesized from both extracts of (a) almond and (b) blackberry. Corresponding deconvoluted patterns of silver nanoparticles for (c) almond and (d) blackberry extracts.

Table 2. Binding energies of the purified silver nanoparticles synthesized from extracts.

Sources	Ag 3d5/2	Ag 3d3/2	AgO	C	N	O
Alm.N.Ext./AgNP	367.15	373.21	368.8	286.66	398.85	532.21
BB.F.Ext./AgNP	367.76	373.81	368.8	285.00	400.00	532.23

The XPS survey spectra (figures 5(a) and (b)) show C, N, O, and Ag atoms with high purity. The binding energy referenced to the standard C1s at 286.60 eV. Results show O1s, C1s, N1s and Ag 3d spectra. The C1s spectra were fitted by one peak at 286 eV corresponding to C-C or C-H vibration for both samples [58]. The corresponding O1s XPS spectrum reveals a peak at 531.2 ± 0.1 eV and is assigned to metal-oxide [59, 60], and the 398.66 eV correspond to N1s (figures 5(a) and (b)). The N1s peak is resolved into two peaks at 398.85 and 400 eV for both the Alm.N.Ext./AgNPs and BB.F.Ext./AgNPs, respectively.

Charged nitrogen atoms with an electrostatic interaction with the silver surface are proved. The peak at 398.85 eV assigned to C–N unit points, therefore, to the interaction between N atoms and the silver nanoparticles. The XPS spectra showed double peaks of low energy bands (Ag 3d5/2) at 367 eV beside the higher energy bands (Ag 3d3/2) at 373 eV. It is comparable to the individual core levels of bulk Ag crystals (368 and 374 eV) [59]. For this reason, the difference in the original structure of the biogenic resources and their respective influences on developing AgNPs are established (table 2). The spectra were fitted in terms of two

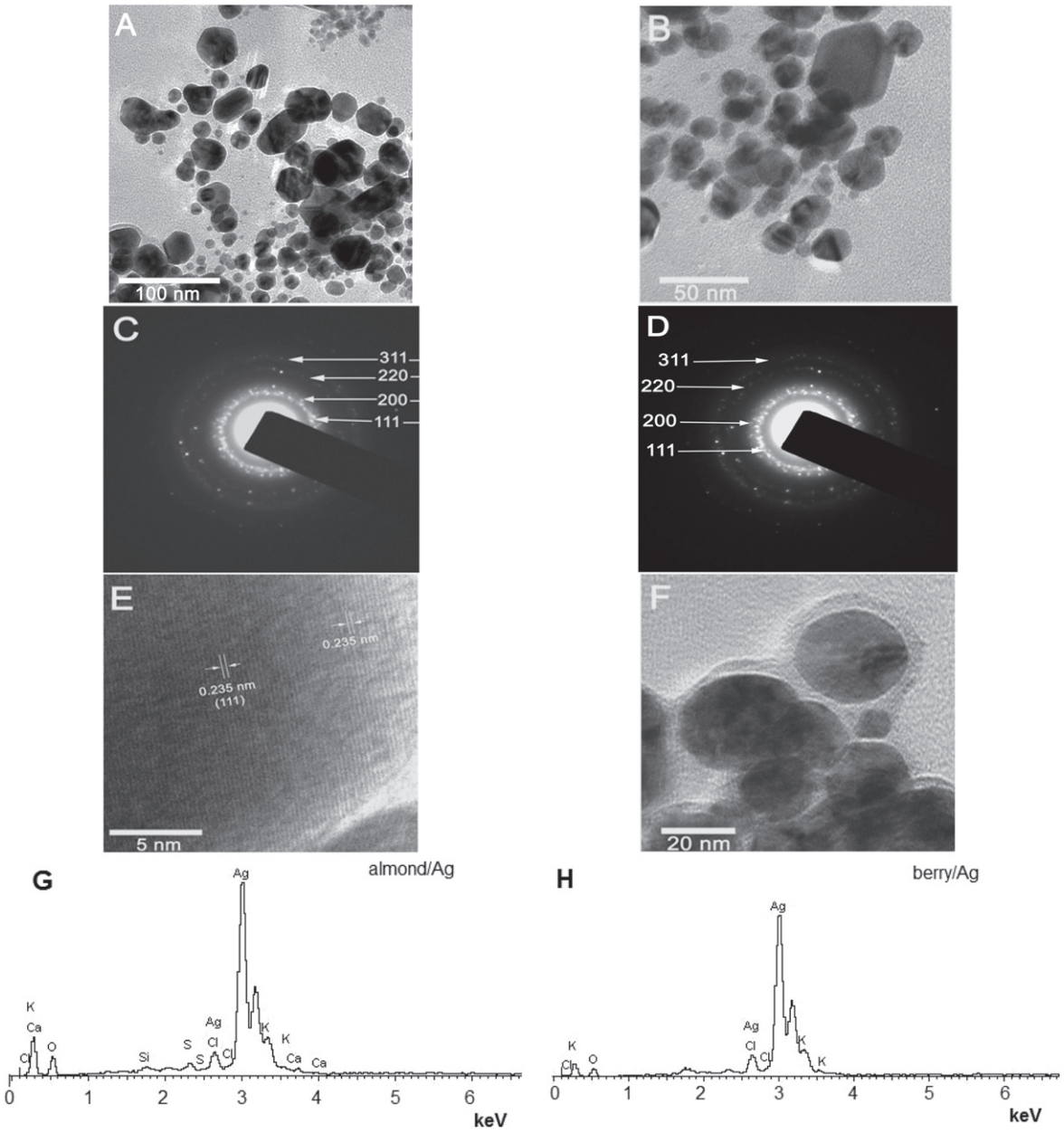

Figure 6. TEM under different magnifications and corresponding EDAX pattern with SAED for almond/Ag ((A), (C), (E), (G)) and for berry/Ag ((B), (D), (F), (H)).

Table 3. Zeta potential and dynamic light scattering values of Ag synthesized from both extracts.

Sample	Mean zeta potential (mV)	Zeta deviation (mV)	Conductivity (ms/cm)	Polydispersity index (PdI)
Alm.N.Ext./AgNP	−31.0	±6.78	0.182	0.727
BB.F.Ext./AgNP	−13.2	±5.97	0.297	0.507

different chemical species with small energy Ag 3d5/2 ~367 eV attributed to metallic silver (Ag^0), coinciding with the literature [60]. The higher energy band at Ag 3d3/2 ~373 eV is assigned to an oxidation state due to heating.

The TEM images of Alm.N.Ext./AgNPs and BB.F.Ext./AgNPs samples are shown in figures 6(A) and (B), respectively. The average particle sizes of the monodispersed silver nanoparticles are 24.5 and 21.5 nm for Alm.N.Ext./AgNPs and BB.F.Ext./AgNPs, respectively. The zeta potential and dynamic light scattering values of Ag synthesized from both extracts were shown in table 3. Single nanocrystal revealed Ag-lattice fringes for almond/Ag (figure 6(E)) while Ag larger grains for berry extract have triangular and hexagonal shapes [61–63]. In addition, energy dispersive x-ray analysis (EDAX) pattern of sample derived from almond extract characteristically approved traces of Ca at 4.0, 3.8 and 0.3

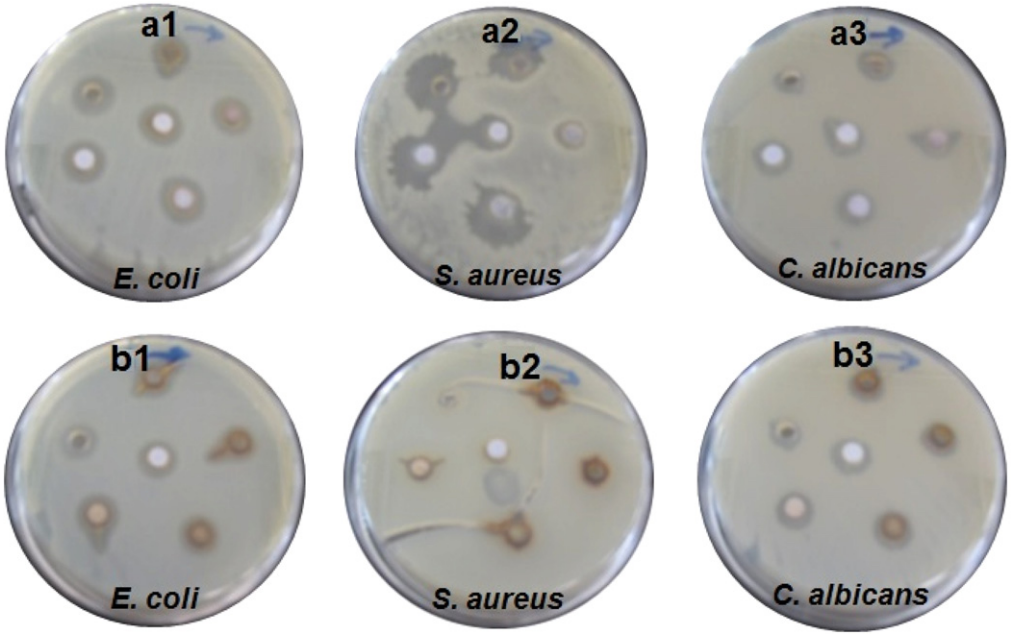

Figure 7. Antimicrobial plates: (a) almond and (b) berry extracts against the three species: 1 for *E. coli*, 2 for *S. aureus* and 3 for *C. albicans*. Six wells in each plate are revealing six different Ag concentrations.

EDX (figure 6(G)) while those for Cl and K appeared at 2.6 and 3.4 keV, respectively. Conversely, elongated rods with high aspect ratios and truncated silver nanoparticles are shown for the blackberry/Ag (figure 6(B)). Additionally, the particles are enveloped by a protective capping film. The selected area electron diffraction (SAED) patterns proved the particles crystallinity with their planes agreeing with corresponding XRD patterns. The strong optical absorption peaks recorded approximately at 3 keV, for both synthesized AgNPs are typically reported for the absorption of elemental silver nanoparticles [64]. Traces of O atoms recorded at 0.6 keV could be due to linked biomolecules. Figure 6(B) shows nanoparticles of increased sizes and different morphologies. The number of the polyhedral particles increased, with few displaying rod forms. The extreme agitation between the molecules should have led to a consequent aggregation of the small particles due to rapid collisions. As the Ag^{+} concentrations were constant for both sources, a higher growth rate of nanoparticles is confirmed within a shorter time in the berry extract. Figure 6 have clear lattice fringes. Few non-spherical polyhedral particles are also recorded, especially for blackberry (figure 6(B)).

These fresh nanocrystals lack the dominance of protective biomolecules leading to anisotropic nanostructures of pentagons, spherical, triangle and hexagon forms. The thin organic layer is acting as a capping agent leading to sound dispersion at macroscopic scale for both, especially in almond.

The antimicrobial activities of ANPs with gradual, incremental concentrations were compared to the synergistic effect of almond and blackberry extracts (figure 7). The three different microorganism reference strains are accused to be significant borne pathogens from animal origin.

Antimicrobial activities of tested biogenic extracts without AgNPs were shown in table 4 and with AgNPs were shown in figure 8.

From table 4 and figure 8 we see that the extracts of almond and berry gave 13.67 and 11.0 mm against *E. coli*, respectively. Therefore, the almond extract is more effective against *E. coli* than the blackberry one. However, in the presence of Ag, the inhibitory zones of the highest concentration of Ag/almond and Ag/blackberry (12.67 against 13.0 mm). Therefore, Ag/berry inhibition is stronger against *E. coli* especially at the maximum concentration (4 mM). The effects of almond and blackberry on *S. aureau, E. coli* and *C. albicans* were estimated as following: for *S. aureus* the almond extract alone is active (16.67 mm inhibition zone) while berry extract has no effect. The highest concentration of Ag (4 mM) provided 15 and 8 mm inhibitory zones for Ag/almond and Ag/berry, respectively. All Ag/Alm concentrations resulted in higher antimicrobial effect except at Ag/almond 2 mM but were still lower than almond extract alone. On the other hand, for the Ag/berry, all levels lead to significant effect, except, the 3 mM give a negative value similar to the extract alone.

For *C. albicans*: almond and berry extracts alone have similar inhibitory effect against mycotic *C. albicans*. Additionally, Ag/almond is equivalent to almond alone, i.e., Ag has a negligible effect at the studied concentrations and against the three species. The lowest Ag concentration having a larger inhibitory zone (11.0 mm) presents an exception. Similarly, berry shows 10.0 mm with 1 and 4 mM Ag concentrations. Whereas, the 2 and 3 mM give 11.0 and 11.33 mm inhibitory zone in the same sequence.

Figure 9 shows the cytotoxicities of the AgNPs synthesized within both extracts were evaluated against two cell lines: human liver hepatocellular carcinoma (HepG2) and

Table 4. Antimicrobial activities of tested biogenic extracts without Ag nanoparticles and its synergistic effects against the tested microbial reference strains (bacterial and mycotic).

		Bacterial strains	Mycotic strains	
Concentration of Ag (mM) in 30 ml Ag/extract	Tested strains / Nanoparticle	Inhibition zone of *E. coli* O157 ATCC 700728 (mm, average)	Inhibition zone of *enterotoxigenic S. aureus* ATCC 13565 (mm, average)	Inhibition zone of *C. albicans* ATCC (mm, average)
1	1 BB	12.00	10.67	10.67
2	2 BB	10.33	8.33	11.00
3	3 BB	10.67	−ve	11.33
4	4 BB	13.00	8.00	10.00
extract	BB	11.00	−ve	10.00
1	1 Alm	14.00	14.33	11.00
2	2 Alm	12.33	9.67	10.00
3	3 Alm	12.67	16.33	9.67
4	4 Alm	12.67	15.00	10.33
extract	Alm	13.67	16.67	10.00

BB = blackberry, Alm = almond, −ve = no inhibition

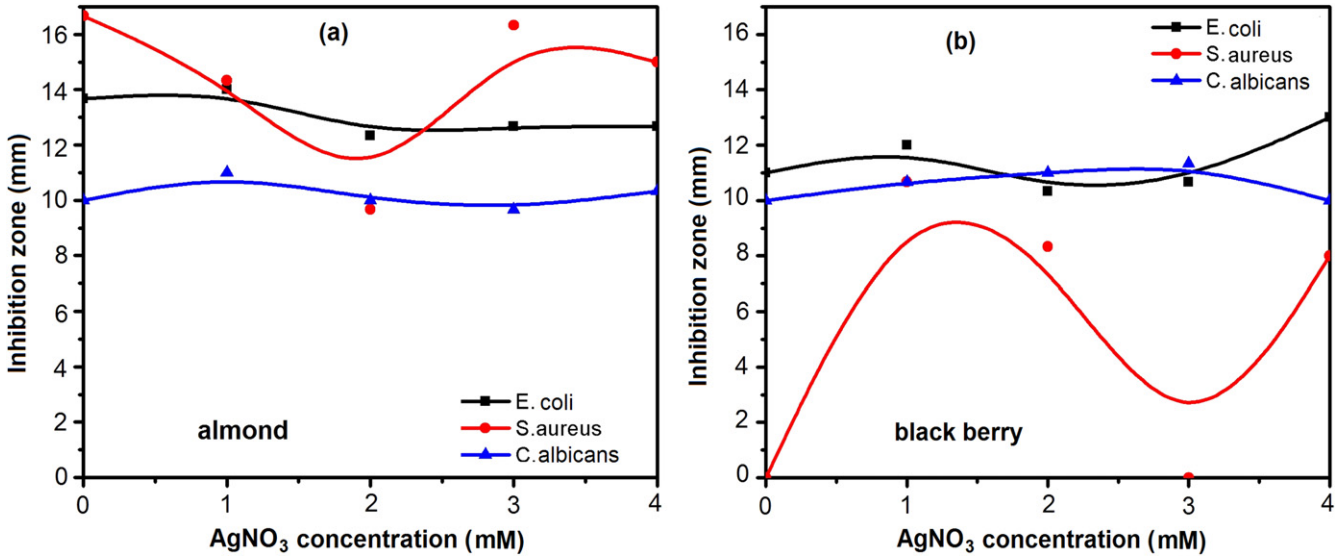

Figure 8. Antimicrobial activities of investigated plant extracts with AgNPs and their synergistic effects against tested microbial reference strains (bacterial and mycotic). Extracts were from (a) almond nuts and (b) blackberry fruits.

human breast adenocarcinoma (MCF7). Initial Ag levels (Alm1 and BB1) are 1 mM. The influence of doubling Ag concentrations on the IC_{50} of the tested cell lines was considered: 2, 3 and 4 are their duplicates, triplicates and quadruple, respectively. The Ag/Alm group showed that any increase in Ag concentration lead to reduced IC_{50} against MCF7. In almond extract and at the highest Ag concentration (4 mM), the yield is only one fifth of the IC_{50} corresponding to 1 mM concentration and is achieved in a continuous manner. A similar trend is recorded for the Ag/BB group except for the 2 mM, whose, IC_{50} is higher than the 1 mM Ag. Comparatively, the Ag/BB is more efficient against MCF7 than Ag/Alm especially at the highest level. Additionally, the 1 and 3 mM of the Ag/BB is better than Ag/Alm while the 2 and 4 mM recorded similar effect against MCF7. Therefore, 4 mM are needed from each Ag/extract to achieve IC_{50} below 10. HePG2 data prove that only two Ag/Alm concentrations (2 and 3 mM) and three concentrations of Ag/BB (1, 3, and 4 mM) proved any gradual increase in Ag concentrations/extract lead to reduced IC_{50} values for Ag/Alm. At particular concentrations of Ag/Alm and Ag/BB, the latter is more efficient against HePG2. Since at 3 mM the IC_{50} of Ag/BB is 32 while it is 42 for Ag/Alm. For both cell lines and at the same concentration of 3 mM of Ag/BB, $IC_{50} = 10$ and 32 against MCF7 and HePG2, respectively. Therefore, the influence of Ag/BB against MCF7 is three times more efficient than HePG2 [65, 66]. (The HePG2 study is to be continued).

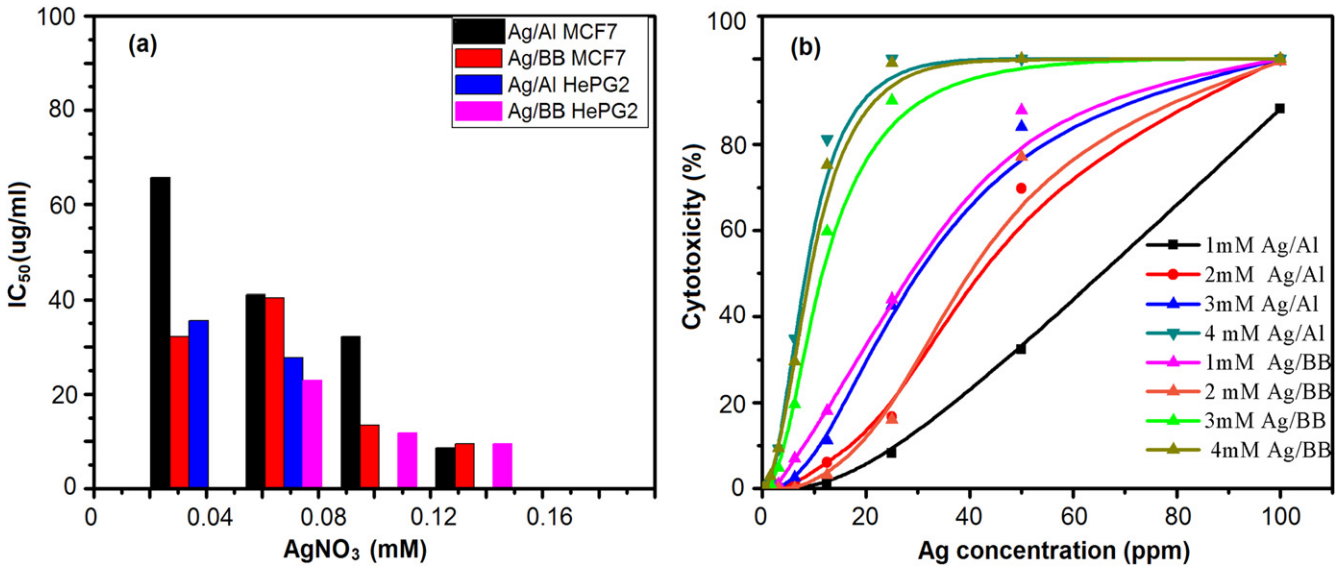

Figure 9. (a) Anticancer activities of investigated plant extracts with Ag nanoparticles and their synergistic effects against hepatocellular carcinoma (HEPG2) and human breast cancer adenocarcinoma (MCF7), (b) cytotoxicity of the AgNPs versus Ag concentration.

The achieved AgNPs have individual orientations. Evidently, the morphology of AgNPs is nearly spherical, with some non-spherical ones having sizes less than 100 nm. Spherical, as well as triangular or hexagonal particles, exhibited enhanced physical properties especially when they are small in size as the antibacterial properties of AgNPs were reported to be size-dependent [65–75]. Comparing, Ag/Alm versus Ag/BB, the former is more efficient against *S. aureus* since, the latter shows better efficiency against *E. coli*. The Ag/Alm particle size is smaller than Ag/BB. Average crystallite sizes of AgNPs is 18 nm and 42 nm for Ag/Alm compared to Ag/BB. Additionally, the polydispersity index of Ag/Alm is 0.727 compared to 0.507 for Ag/BB. Moreover, the higher stability of the former (−31.0) compared to only one-third of this value (−13.2 mV) for the later, is explaining, therefore, the stronger antibacterial effect. Verifying FTIR results, the presence of carbonyl triglycerides, fatty acids and vitamin E in almond are more effective than the phenolic compound in berry. Similarly, such trend could be drawn.

4. Conclusions

A simple and cost efficient route to synthesize stable and mono-dispersed AgNPs was obtained from green microwave extracts of almond nuts and blackberry fruits. C-H groups of almond/extract are responsible for Ag ionic reduction into Ag^0 nanoparticles while the O-H groups of berry fruits played the reduction role. Berry extract affected growth rate of AgNPs within a shorter time. The higher stability of almond AgNPs compared to berry AgNPs was proved by PDI data. The green extracts protected the nanoparticles against aggregation, therefore, excluded the need for capping agents. The AgNPs crystallinity is confirmed by EDAX and XPS, with the appearance of C, O and N proving the extracellular organic moieties enveloping the AgNPs. As a result, their involvement in the reduction process is ensured. The achieved results revealed significant synergistic effect of the extracts (blackberry and almond) and AgNPs.

The most effective bacterial inhibition was achieved by *S. aureus* followed by *E. coli*, and the least was *C. albicans* for Ag/almond. Conversely, antimicrobial functions of Ag/berry followed the order gram-negative bacteria *E. coli* better than *C. albicans* with the least hindrance activity by the gram-positive strain *S. aureus*. Conclusively, no linear correlation is observed between Ag concentrations and inhibitory zone diameters against the three antimicrobial species. While, on the contrary, differences in efficiency of the Ag/extracts against the three studied species is proved. The smaller particle sizes of Ag/almond, the higher PDI, UV- stability and triple zeta potential values are in favor of such hindrance. The anti-cancerous influence of Ag/berry was stronger against (HepG2) and (MCF7) breast cancer. For this reason, the present results established multiple beneficial functions of naturally occurring antioxidant polyphenols to human health providing adequate anticancer capabilities in a dose-dependent manner. The current study was performed to add scientific contribution in regard to the use of AgNP in nanomedicine.

Acknowledgments

The financial support of the National Research Centre to the present project within the framework of the 10TH project round 2013–2016 ‘Noble metal/chitosan/phosphatic composite hydrogels with antibacterial/anticancer functions as bone repair for minimum invasive surgeries’ is appreciated. Thanks are due to Dr Tarek A El-kholy, Biomaterials Department for his help during TEM investigations.

References

[1] Glomm R W 2005 *J. Disper. Sci. Technol.* **26** 389
[2] Basavaraja S, Balaji S D, Lagashetty A, Rajas A H and Venkataraman A 2008 *Mater. Res. Bull.* **43** 1164
[3] Smith N and Lane N 2000 *National Nanotechnology Initiative: Leading to the Next Industrial Revolution* (Washington DC: National Science and Technology Council NSTC)
[4] Ahmad A, Mukherjee P, Senapati S, Mandal D, Khan M I, Kumar R and Sastry M 2003 *Colloid Surface* B **27** 313
[5] Darroudi M, Ahmad M B, Abdullah A and Azowa Ibrahim N 2011 *Int. J. Nano Med.* **6** 677
[6] Park H H and Choi Y J 2011 *Thin Solid Films* **519** 6214
[7] Hubenthal F 2011 Noble metal nanoparticles: synthesis and optical properties *Comprehensive Nanoscience and Technology* ed D L Andrews, G D Scholes and G P Wiederrecht (Amsterdam: Elsevier Science & Technology) p 375
[8] Jin E S, Ghodake G S, Deshpande N G and Lee Y P 2010 *Colloids Surface* B **75** 584
[9] Sanghi R and Verma P 2009 *Bioresour. Tech.* **100** 501
[10] Kouvaris P, Delimitis A, Zaspalis V, Papadopoulos D, Tsipas S A and Michailidis N 2012 *Mat. Lett.* **76** 18
[11] Anastas P T and Warner J C 1988 *Green Chemistry: Theory and Practice* (Oxford: Oxford University Press)
[12] Kappe C O 2004 *Angew. Chem. Int. Edit.* **26** 6250
[13] Roberts B A and Strauss C R 2005 *Chem. Res.* **38** 653
[14] Das R, Mehta D and Bhardawaj H 2012 *Int. J. Res. Devel. Pharm. Life Sci.* **1** 32
[15] García-Lopes C, Grané-Teruel N, Berenguer-Navarro V, Garcia-Garcia J E and Martín-Carratala M L 1996 *J. Agr. Food Chem.* **44** 175
[16] Romojaro F E, GarcíaLópez J and Andreu F J 1977 *Anal. Edafol. Agrobiol.* **36** 121
[17] Jaceldo-Siegl K, Sabaté J, Rajaram S and Fraser G E 2004 *Br. J. Nutr.* **92** 533
[18] Serra N P, Adams LS, Zhang Y, Lee R, Sand D, Schiller H S and Heber D J 2006 *J. Agr. Food Chem.* **54** 9329
[19] Seeram N P 2008 *J. Agr. Food Chem.* **56** 627
[20] Heather M A C, Michael H and Jenny M W 2003 *J. Med. Food* **6** 57
[21] Katsura N, Iwashita K, Tsuchida T, Kobori M and Yamaki K 2003 *J. Agr. Food Chem.* **51** 68
[22] Giovanelli G and Buratti S 2009 *Food Chem.* **112** 903
[23] Prior R L *et al* 1998 *J. Agr. Food Chem.* **46** 2686
[24] Mullen W, Lean M E J and Crozier A 2002 *J. Chromatogr.* A **966** 63
[25] Anttonen M J and Karjalainen R O 2005 *J. Food Compos. Anal.* **18** 759
[26] Zhang L, Li J, Hogan S, Chung H, Welbaumge E and Zhou K 2009 *Food Chem.* **119** 592
[27] Daniel E M, Krupnick A S, Heur Y-H, Blinzler J A, Nims RW and Stoner GD 1989 *J. Food Comp. Anal.* **2** 338
[28] Gross W G 1994 *Diseases Due to Escherichia Coli in Poultry* ed C L Gyles (Wallingford, UK: CAB International) p 237
[29] Nataro J P and Kaper J B 1998 *Clin. Microbiol. Rev.* **11** 142
[30] White D G 2005 *Antimicrobial Resistance in Bacteria of Animal Origin* ed F M Aarestrup (Washington DC: ASM Press) p 145
[31] Guven K, Mutlu B M, Gulbandilar A and Cakir P 2010 *J. Food Safety* **30** 196
[32] Aydin A, Muratoglu K, Sudagidan M, Bostan K, Okuklu B and Harsa S 2011 *Foodborne Pathogens and Disease* **8** 63
[33] Nagarajappa S, Thakur M S and Manonmani H K 2012 *J. Food Safety* **32** 59
[34] Bergdoll M S and Robbins R N 1973 *J. Milk Food Technol.* **36** 610
[35] Tarfarosh M A and Purohit S K 2008 *Vet. Scan* **3** 14
[36] Spanamberg A, WünderJr E A, Brayer Pereira D I, Argenta J, CavalliniSanches E M, Valente P and Ferreiro L 2008 *Rev. Iberoam. Micol.* **25** 154
[37] Seker E 2010 *Mycopathologia* **169** 303
[38] Krukowski H, Tietze M, Majewski T and Rózański P 2000 *Poland Mycopathologia* **150** 5
[39] Perez V, Corpa J M, Garcia Marin J F, Aduriz J J and Jensen H E 1999 *J. Vet. Med.* B **46** 613
[40] Guirguis O W, Abd Elkader M F H and Nasrat A A 2013 *Mater. Lett.* **93** 353
[41] Zawrah M F and Abd El-Moez Sherein I 2011 *Life Science J.* **8** 37
[42] Sgouras D, Maragkoudakis P, Petraki K, Martinez-Gonzalez B, Eriotou E, Michopoulos S, Kalantzopoulos G, Tsakalidou E and Mentis A 2004 *Microbiol.* **70** 518
[43] Elumalai E K, Prasad T N V K V, Hemachandran J, Vivian S, Therasa S, Thirumalai T and David E 2010 *J. Pharm. Sci. Res.* **2** 549
[44] Jaidev L R and Narasimha G 2010 *Colloid. Surf.* **81** 430
[45] Lopez-Salido I, Lim D C and Kim Y D 2005 *Surf. Sci.* **588** 6
[46] Philip D 2010 *Physica* E **42** 1417
[47] Mujeeb K, Merajuddin K, Syed F A, Muhammad N T, Wolfgang T, Hamad Z A, Al-Hartman A, Mohammed R and Siddiqui H 2013 *Int. J. Nanomed.* **8** 1507
[48] Jongho K, Sang W K and Yong S K 2008 *Colloid. Surf.* A **320** 189
[49] Sanahuja A B, Moya M S P, Perez S E M, Teruel NG and Carratala M L M 2009 *J. Am. Oil Chem. Soc.* **86** 51
[50] Csanádi Z S, Serjési P C, Nemestóthy N and Bélafi-BaKó K 2012 *Acta Aliment.* **41** 94
[51] Kacurakova M, Capek P, Sasinkova V, Weller N and Ebringerova A 2000 *Carbohyd. Polym.* **43** 195
[52] Kumar A D 2012 *Int. Res. J. Pharm.* **3** 169
[53] Lai Y, Zhuang H, Xie K, Gong D, Tang Y and Sun L 2010 *New J. Chem.* **34** 1335
[54] Prakash P, Gnanaprakasam P, Emmanuel R, Arokiyaraj S and Saravanan M 2013 *Colloid. Surf.* B **108** 255
[55] Pilar P, Valentin N, Khalid N, Munetaka O, Abd-Lefdil M and Raquel D 2012 *Appl. Surf. Sci.* **258** 8807
[56] Carroll K L, Reveles J U, Shultz M D, Khanna S N and Carpenter E E 2011 *J. Phys. Chem.* C **115** 2656
[57] Manivel P, Balamurugan A, Ponpandian N, Mangalaraj D and Viswanathanm C 2012 *Spectrochim. Acta* A **95** 305
[58] Min-Kyu J and Misook K 2008 *Mater. Lett.* **62** 676
[59] Zhang Z, Zhang X, Xin Z, Deng M, Wen Y and Song Y 2011 *Nanotechnology* **22** 21
[60] Sharma J, Chaki N K, Mandale A B, Pasricha R and Vijayamohanan K 2004 *J. Colloid Interface Sci.* **272** 145
[61] ISO 13321 1996 Particle size analysis—Photon correlation spectroscopy
[62] Sumesh E, Bootharaju M S and Pradeep A T 2011 *J. Hazard Mater.* **189** 450
[63] Chen M S F, Xiaohui Y, Yingjie D, Yingna X, Heming X, Wenji Z, Shuangshuang S, Li A, Naixian Z and Weiss P 2013 *Int. J. Nanomed.* **8** 4045
[64] Mouxing F U, Qingbiao L I, Daohua S U N, Yinghua L U, Ning H E, Deng X U, Wang H and Huang J 2006 *Chinese J. Chem. Eng.* **14** 114
Kumara K M, Sinhaa M, Mandala B K, Ghoshb A R, Kumarc K S and Reddy P S 2012 *Spectrochem. Acta* A **91** 228
[65] Altankov G, Richard K and Groth T 2003 *Mater.wiss. Werkst. tech.* **34** 1120
[66] Tomaszewska E, Soliwoda K, Kadziola K, Tkacz-Szczesna B, Celichowski G, Cichomski M, Szmaja W and Grobelny J 2013 *J. Nanomater.* **2013** 1
[67] Vidhu V K, Aromal S A and Philip D 2011 *Spectrochim. Acta* A **83** 392

[68] Mohamed M S, Awad Y E E D, El-Hallouty S M and El-Araby M 2012 *Open J. Med. Chem.* **2** 78
[69] Hassan G S, El-Messery S M, Al-Omary F A, Al-Rashood S T, Shabayek M I, Abulfadl Y S and El-Subbagh H I 2013 *Eur. J. Med. Chem.* **66** 135
[70] Li S, Zhang Y Y V, Xu J and Zhang L N 2011 *Biomacromolecules* **12** 2864
[71] Hunter RJ 1998 *Zeta Potential in Colloid Science: Principles and Applications* (London: Academic)
[72] Wang C, Ma J, Cheng W and Zhang R 2002 *Mater. Lett.* **57** 99
[73] Siliva F C, Santos A B, De Carvalho T M and De Souza J 1987 *Leuk. Biol.* **41** 143
[74] Tadas S S, Devin G B, Ran Z, King Hang A L and Philip B M 2013 *Angew. Chem. Int. Ed.* **52** 10766
[75] Shameli K, Bin Ahmad M, Jazayeri S D, Shabanzadeh P, Sangpour P, Jahangirian H and Gharayebi Y 2012 *Chem. Central J.* **6** 73